Check for updates

The FERM protein EPB41L5 regulates actomyosin contractility and focal adhesion formation to maintain the kidney filtration barrier

Christoph Schell[a,b,1,2], Manuel Rogg[b,1], Martina Suhm[b,1], Martin Helmstädter[b], Dominik Sellung[b], Mako Yasuda-Yamahara[b,c], Oliver Kretz[b,d,e], Victoria Küttner[f,3], Hani Suleiman[g], Laxmikanth Kollipara[h], René P. Zahedi[h], Albert Sickmann[h,i,j], Stefan Eimer[d,k], Andrey S. Shaw[g], Albrecht Kramer-Zucker[b], Mariko Hirano-Kobayashi[l,4], Takaya Abe[m], Shinichi Aizawa[m], Florian Grahammer[b,e], Björn Hartleben[b,5], Jörn Dengjel[d,f,k,n], and Tobias B. Huber[b,d,k,e,2]

[a]Institute of Surgical Pathology, Medical Center - University of Freiburg, Faculty of Medicine, University of Freiburg, 79106 Freiburg, Germany; [b]Department of Medicine IV, Medical Center - University of Freiburg, Faculty of Medicine, University of Freiburg, 79106 Freiburg, Germany; [c]Department of Medicine, Shiga University of Medical Science, Otsu, Shiga 522-8522, Japan; [d]BIOSS Centre for Biological Signalling Studies, Albert-Ludwigs-University Freiburg, 79106 Freiburg, Germany; [e]III. Medizinische Klinik, Universitätsklinikum Hamburg-Eppendorf, 20251 Hamburg, Germany; [f]Department of Dermatology, Faculty of Medicine, Medical Center, University of Freiburg, 79106 Freiburg, Germany; [g]Department of Pathology, Washington University in St. Louis, MO 63130; [h]Leibniz-Institut für Analytische Wissenschaften – ISAS – e.V., 44139 Dortmund, Germany; [i]Department of Chemistry, College of Physical Sciences, University of Aberdeen, Aberdeen AB24 3FX, Scotland, United Kingdom; [j]Medizinische Proteom-Center, Ruhr-Universität Bochum, 44801 Bochum, Germany; [k]Center for Biological Systems Analysis (ZBSA) and Freiburg Institute for Advanced Studies, Albert-Ludwigs-University, 79106 Freiburg, Germany; [l]Laboratory for Vertebrate Body Plan, Center for Developmental Biology, RIKEN Kobe, Kobe 650-0047, Japan; [m]Genetic Engineering Team, RIKEN Center for Life Science Technologies, Kobe 650-0047, Japan; and [n]Department of Biology, University of Fribourg, 1700 Fribourg, Switzerland

Edited by Martin R. Pollak, Harvard University, Beth Israel Deaconess Medical Center, Brookline, MA, and approved April 27, 2017 (received for review October 27, 2016)

Podocytes form the outer part of the glomerular filter, where they have to withstand enormous transcapillary filtration forces driving glomerular filtration. Detachment of podocytes from the glomerular basement membrane precedes most glomerular diseases. However, little is known about the regulation of podocyte adhesion in vivo. Thus, we systematically screened for podocyte-specific focal adhesome (FA) components, using genetic reporter models in combination with iTRAQ-based mass spectrometry. This approach led to the identification of FERM domain protein EPB41L5 as a highly enriched podocyte-specific FA component in vivo. Genetic deletion of *Epb41l5* resulted in severe proteinuria, detachment of podocytes, and development of focal segmental glomerulosclerosis. Remarkably, by binding and recruiting the RhoGEF ARGHEF18 to the leading edge, EPB41L5 directly controls actomyosin contractility and subsequent maturation of focal adhesions, cell spreading, and migration. Furthermore, EPB41L5 controls matrix-dependent outside-in signaling by regulating the focal adhesome composition. Thus, by linking extracellular matrix sensing and signaling, focal adhesion maturation, and actomyosin activation EPB41L5 ensures the mechanical stability required for podocytes at the kidney filtration barrier. Finally, a diminution of EPB41L5-dependent signaling programs appears to be a common theme of podocyte disease, and therefore offers unexpected interventional therapeutic strategies to prevent podocyte loss and kidney disease progression.

focal adhesion | actomyosin | podocyte | FSGS

Glomerular epithelial cells or podocytes represent a pericyte-like cell type establishing the kidney filtration barrier in combination with endothelial cells and the basement membrane (1, 2). These cells exhibit a strictly polarized morphology characterized by a large cell body and extending primary and secondary foot processes, which enclose glomerular capillaries (3). The slit diaphragm, a specialized and unique cell–cell contact, connects interdigitating foot processes and confines the basolateral membrane compartment of podocytes (2, 4).

Because of the constant exposure of podocytes to filtration forces, tight adherence to the basement membrane is required to prevent detachment into Bowman's capsule. As a consequence, loss of podocytes from the glomerular basement membrane (GBM) is a major contributing factor to the progression of glomerular and chronic kidney disease (5–7).

On a molecular level, a multitude of adhesion receptors including heterodimeric integrins mediate interaction of cells with the surrounding extracellular matrix (ECM) or the basement membrane (8, 9). Integrin receptors are linked to an intracellular multiprotein complex, collectively named the integrin adhesome, constituting various adaptor proteins, GTPases, kinases, and phosphatases (9). One common form of integrin-mediated adhesion is focal adhesions (FAs), which have been extensively studied in cultured cells (9). Functionally, FAs support the physical interaction of cells to the ECM, establish connection to the actomyosin

Significance

Loss of podocyte adhesion is a hallmark of glomerular disease progression. Here we unravel the in vivo composition of the podocyte adhesion machinery by the use of quantitative proteomics and identify the FERM domain protein EPB41L5 as a selectively enriched novel podocyte focal adhesion protein. EPB41L5 is essential to maintaining podocyte adhesion in vivo by recruiting the Rho GEF ARHGEF18, initiating a signaling cascade and ultimately resulting in increased actomyosin activity and focal adhesion stabilization. As EPB41L5 is down-regulated in various glomerular pathologies, these findings offer a perspective for interventions aiming to prevent loss of podocytes in glomerular disease.

Author contributions: C.S., M.R., and T.B.H. designed research; C.S., M.R., M.S., M.H., D.S., M.Y.-Y., O.K., H.S., L.K., R.P.Z., and B.H. performed research; V.K., L.K., R.P.Z., A.S., S.E., A.S.S., A.K.-Z., M.H.-K., T.A., S.A., F.G., and J.D. contributed new reagents/analytic tools; C.S., M.R., H.S., and J.D. analyzed data; and C.S., M.R., and T.B.H. wrote the paper.

The authors declare no conflict of interest.

This article is a PNAS Direct Submission.

Freely available online through the PNAS open access option.

[1]C.S., M.R., and M.S. contributed equally to this work.

[2]To whom correspondence may be addressed. Email: t.huber@uke.de or christoph.schell@uniklinik-freiburg.de.

[3]Present address: Cold Spring Harbor Laboratory, Cold Spring Harbor, NY 11724.

[4]Present address: Vascular Biology Program, Boston Children's Hospital and Harvard Medical School, Boston, MA 02115.

[5]Present address: Institut für Pathologie, Medizinische Hochschule Hannover, Hannover 30625, Germany.

This article contains supporting information online at www.pnas.org/lookup/suppl/doi:10.1073/pnas.1617004114/-/DCSupplemental.

cytoskeleton, and provide a signaling hub to fine-tune regulatory cascades and cellular functions. The clinical relevance of the adhesome for podocyte function was recently demonstrated by the identification of mutations in the *Integrin alpha3* gene, causing glomerular and skin disease in affected patients (10). In addition, other focal adhesome components such as INTEGRIN-beta1 and INTEGRIN-LINKED KINASE (ILK), as well as other core focal adhesome components, were identified to be critical for podocyte maintenance (11–15).

Despite those previous advances, there is still no unifying pathophysiological concept of the role of FAs in podocyte biology, allowing for the design of targeted diagnostic, as well as therapeutic, approaches. In addition, a comprehensive description of podocyte-specific focal adhesome components is still lacking. To identify cell-specific adhesome modulators, we developed a method for large-scale isolation of highly purified podocyte cell populations from murine glomeruli (16). Using iTRAQ-based quantitative MS technology, we developed an unprecedented in vivo description of almost 3,500 podocyte proteins. We used these data and applied bioinformatic filtering approaches to identify components of the podocyte FA complex. This approach enabled the identification of the FERM-domain protein EPB41L5. Characterization of this podocyte-specific molecule offered unexpected insights into the biology, function, and disease mechanism of the kidney filtration barrier.

Results

Analysis of the Podocyte-Enriched Adhesome Identifies FERM-Domain Protein EBP41L5 as a Podocyte-Specific FA Component. One key feature of podocytes is the tightly regulated adhesion to the glomerular basement membrane (Fig. 1*A*) to maintain the filtration barrier (6). Detachment of podocytes from the glomerular basement membrane is a common hallmark of late-stage glomerular disease (Fig. 1*B*), suggesting an involvement of adhesome components (*SI Appendix*, Fig. S1). FAs are multiprotein complexes that sense the ECM environment, integrate incoming signals, and mediate required contractile forces for adhesion adjustment (Fig. 1*D*) (9). To identify podocyte adhesome-associated proteins, we made use of a genetically encoded reporter mouse system (Fig. 1*C*). After FACS sorting, GFP$^+$ podocyte cell populations were subjected to iTRAQ-based quantitative mass spectrometry (Fig. 1*C*). We identified nearly 3,500 proteins using this approach, and ranked those according to their detection rates (relative to nonpodocyte cells; Dataset S1). Pathway and process analysis revealed a high enrichment of integrin-mediated-signaling-associated proteins in podocytes compared with the nonpodocyte fraction (Fig. 1*E*, *SI Appendix*, Fig. S2, and Dataset S1). After selection for enriched proteins, a filtering step for FA gene ontology terms was implemented, resulting in a list of 56 enriched, presumptive FA proteins. In addition to previously described integrins (ITGA3, ITGB5, and ITGAV) and well-established actin-cross-linkers such

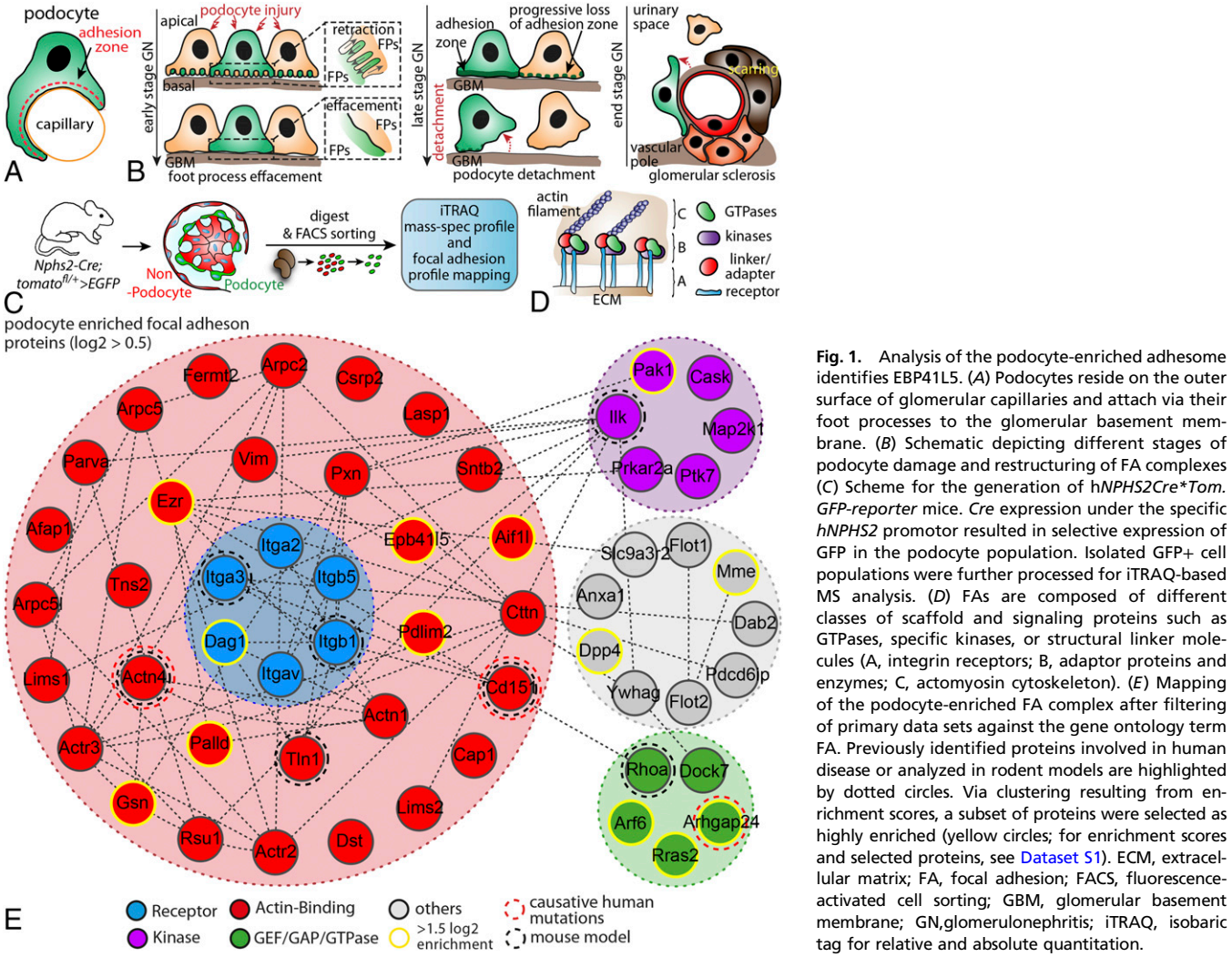

Fig. 1. Analysis of the podocyte-enriched adhesome identifies EBP41L5. (*A*) Podocytes reside on the outer surface of glomerular capillaries and attach via their foot processes to the glomerular basement membrane. (*B*) Schematic depicting different stages of podocyte damage and restructuring of FA complexes (*C*) Scheme for the generation of h*NPHS2Cre*Tom.GFP-reporter* mice. *Cre* expression under the specific *hNPHS2* promotor resulted in selective expression of GFP in the podocyte population. Isolated GFP+ cell populations were further processed for iTRAQ-based MS analysis. (*D*) FAs are composed of different classes of scaffold and signaling proteins such as GTPases, specific kinases, or structural linker molecules (A, integrin receptors; B, adaptor proteins and enzymes; C, actomyosin cytoskeleton). (*E*) Mapping of the podocyte-enriched FA complex after filtering of primary data sets against the gene ontology term FA. Previously identified proteins involved in human disease or analyzed in rodent models are highlighted by dotted circles. Via clustering resulting from enrichment scores, a subset of proteins were selected as highly enriched (yellow circles; for enrichment scores and selected proteins, see Dataset S1). ECM, extracellular matrix; FA, focal adhesion; FACS, fluorescence-activated cell sorting; GBM, glomerular basement membrane; GN,glomerulonephritis; iTRAQ, isobaric tag for relative and absolute quantitation.

as ACTININ-4, we identified recently discovered GTPase modulators such as ARHGAP24 (Fig. 1*E*) (17). We further refined our initial list by integrating recently published experimental data (18) and ended up with a list of 182 potential podocyte-enriched FA proteins (Dataset S1). EPB41L5 appeared as the top enriched protein in our candidate approach after applying different filtering steps for FA-associated protein domains (Dataset S1).

EPB41L5 Localizes to FAs in Vivo. To validate results of our proteome approach, we used mRNA in situ hybridization to develop a specific expression profile for the top candidate *Epb41l5* during murine development. Prenatally, *Epb41l5* expression was restricted to the brain, lung, and kidney (Fig. 2*A* and *SI Appendix*, Fig. S3). In the kidney, expression was particularly strong in the glomeruli at embryonic stage E14.5 (embryonic day 14.5) (Fig. 2*A* and *SI Appendix*, Fig. S3). Immunofluorescence of EPB41L5 further confirmed this expression in rodent as well as human podocytes (*SI Appendix*, Fig. S3). Glomerular epithelial cells undergo a dramatic change in cellular morphology during development (19, 20). To specifically localize EPB41L5 during this polarization process, we used a set of well-established polarity markers in combination with EPB41L5. Here, EPB41L5 showed a predominant colocalization with the basolateral marker SCRIBBLE, but not with the apical marker PODOCALYXIN or the tight junction marker PAR3 (*SI Appendix*, Fig. S4) (21). Using immunogold electron microscopy confirmed that bona fide FA components such as PAXILLIN and ZYXIN predominantly localized at a basal position of podocyte foot processes (Fig. 2 *B–D*). EPB41L5 showed an overlapping localization pattern in close proximity to the glomerular basement membrane (Fig. 2 *E* and *F*). Recently, the super resolution microscopy technique stochastic optical reconstruction microscopy was successfully applied to visualize the nanoscale composition of the glomerular basement membrane (22). Using this technique enabled the detection of EPB41L5 colocalizing with the bona fide FA component INTEGRIN-beta1, whereas no overlap was detectable with the apical marker protein PODOCALYXIN (Fig. 2 *G–L*). Altogether, these different imaging modalities highlight the basolateral, typical FA localization pattern for EPB41L5 in vivo. Remarkably, an altered localization and coarse intensity pattern was detected in biopsy samples from human patients with focal segmental glomerulosclerosis or diabetic nephropathy for EPB41L5 (*SI Appendix*, Fig. S5). These observations were furthermore corroborated by mRNA expression analysis for respective disease entities from open source databases, as well as experimental mouse models (*SI Appendix*, Figs. S5 and S6). Altogether, these data indicate that EPB41L5 is a highly sensitive FA component of podocytes and appears also to be drastically affected in human glomerular disease entities.

Loss of *Epb41l5* Causes Nephrotic Syndrome, Renal Failure, and Lethality. To test for the functional relevance of the loss of *Epb41l5* expression, we generated a conditional knockout model

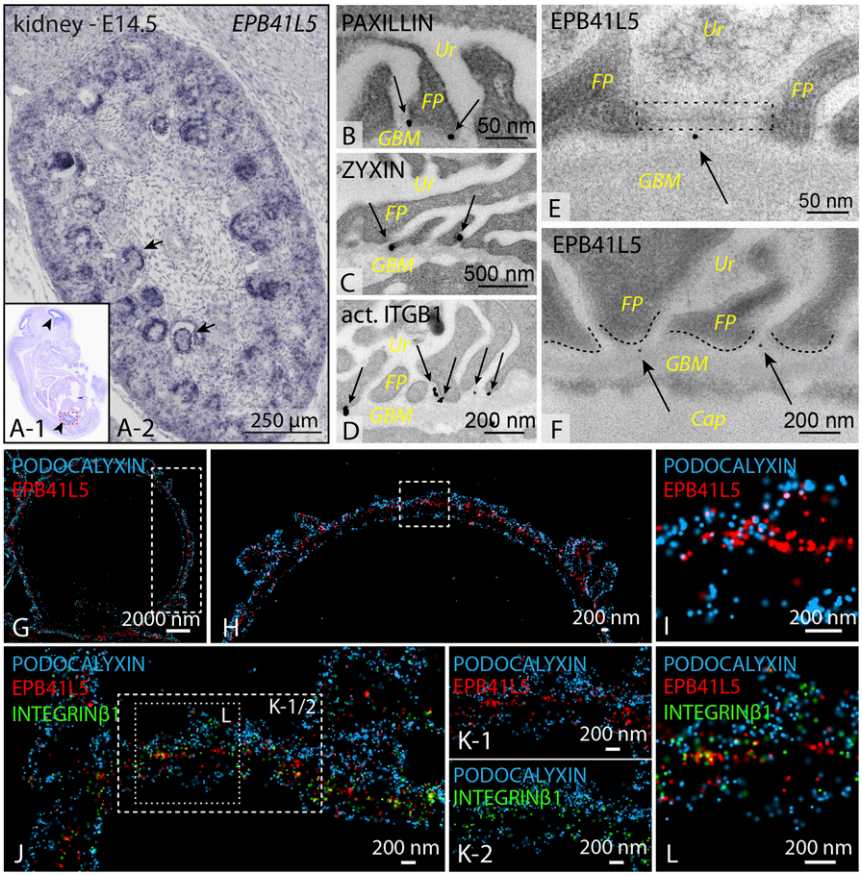

Fig. 2. EPB41L5 localizes at FAs in vivo. (*A*) In situ hybridization revealed that Epb41l5 is exclusively expressed in developing glomeruli of the kidney at embryonic stages E14.5. (*B–F*) Immunogold electron microscopy for core FA components revealed predominant basal localization toward the GBM in wild-type mice. EPB41L5 concordantly localized basally of foot processes. Ur, urinary pole; FP, foot processes; GBM, glomerular basement membrane; Cap, capillary; arrows, gold particles; dotted lines, FP morphology. (*G–L*) Stochastic optical reconstruction microscopy of glomeruli, using PODOCALYXIN (apical marker) and INTEGRIN-beta1 (basal marker) in combination with EPB41L5, demonstrated close proximity and colocalization of EPB41L5 with the FA compartment (as indicated by ITGB1; boxed regions indicate areas of zoomed details).

using standardized loxP technique (Fig. 3 *A–D* and *SI Appendix*, Fig. S7). Glomerular epithelial cells contribute to the maintenance of the kidney filtration barrier, and levels of proteinuria represent a sensitive readout system in terms of podocyte function (2). Analysis of *Epb41l5*$^{fl/fl}$**NPHS2Cre* animals revealed severe proteinuria indicated by albumin/creatinine ratios greater than 100 compared with wild-type animals. Proteinuria in those mice was already present at birth and remained at high levels for the whole observational period (Fig. 3*E*). As a result of high-grade proteinuria and progressing renal failure (as demonstrated by pronounced glomerulosclerosis; Fig. 3 *J* and *K* and *SI Appendix*, Fig. S8), respective knockout animals showed decreased weight gain compared with control animals (Fig. 3*F*). The severe phenotype in terms of proteinuria resulted in premature death of *Ebp41l5* knockout animals, reflected by dramatically reduced survival by 50% 2 wk after birth (Fig. 3*G*). Morphological analysis of kidney sections revealed dilated tubules with an accumulation of proteinaceous casts, reflecting severe proteinuria in knockout animals (Fig. 3 *H–K* and *SI Appendix*, Fig. S8). Given the basolateral localization of EPB41L5 in glomerular epithelial cells, we sought to directly determine the potential influence of EPB41L5 on podocyte cell morphology. Although in wild-type animals, interdigitating FPs were regularly separated by slit diaphragms, *Epb41l5* knockout podocytes displayed a global fusion of FPs at P0 (*SI Appendix*, Fig. S9). Furthermore, slit diaphragms were either not detectable or dislocated to a more apical position (*SI Appendix*, Fig. S9), but there were no obvious changes in apico-basal compartmentalization (*SI Appendix*, Fig. S10). Strikingly, massive podocyte detachment was detectable in *EPB41L5* knockout animals, as demonstrated by decreased numbers of podocytes per glomerulus, as well as increased levels of detached podocytes in the urine (Fig. 3 *L–O* and *SI Appendix*, Fig. S10). To test the effect of EPB41L5 in already completely maturated podocytes, the conditional EPB41L5 floxed allele was intercrossed to a podocyte-specific, doxycycline-dependent inducible *Cre*-system (*SI Appendix*, Fig. S11 and S12). Induction of *Cre*-activity was performed in 4-wk-old animals for a period of 2 wk (*SI Appendix*, Fig. S11). Remarkably, 1 wk after induction, increased levels of proteinuria already were detectable in knockout animals (*SI Appendix*, Fig. S11). In agreement with the *NPH2Cre* line, inducible knockout animals developed signs of progressive focal segmental sclerosis and foot process effacement (*SI Appendix*, Fig. S11 and S12). These alterations were accompanied by altered localization and decreased signal intensity for NEPHRIN, PODOCIN, and SNYAPTOPODIN, whereas the polarity molecule PAR3 exhibited no significant changes (*SI Appendix*, Fig. S12). Together, these findings underline the uttermost importance of EPB41L5 for developing, as well as fully maturated, podocytes in vivo.

To gain mechanistic insights into EPB41L5 function in podocytes, we used a recently established method for isolation of primary podocytes from control and EPB41L5-deficient animals (Fig. 1*C*) (23). As expected, EPB41L5 displayed on a subcellular level a typical FA localization pattern close to the cell border (Fig. 3*P*). Interestingly, a pronounced decrease in migratory function was detected in primary knockout podocytes when seeded on collagen IV coated surfaces (*SI Appendix*, Fig. S13).

EPB41L5 Controls FA Maturation and Cellular Spreading. Because primary podocytes are only of limited availability, we used CRISPR/Cas9 genome editing technology to generate *EPB41L5*-deficient

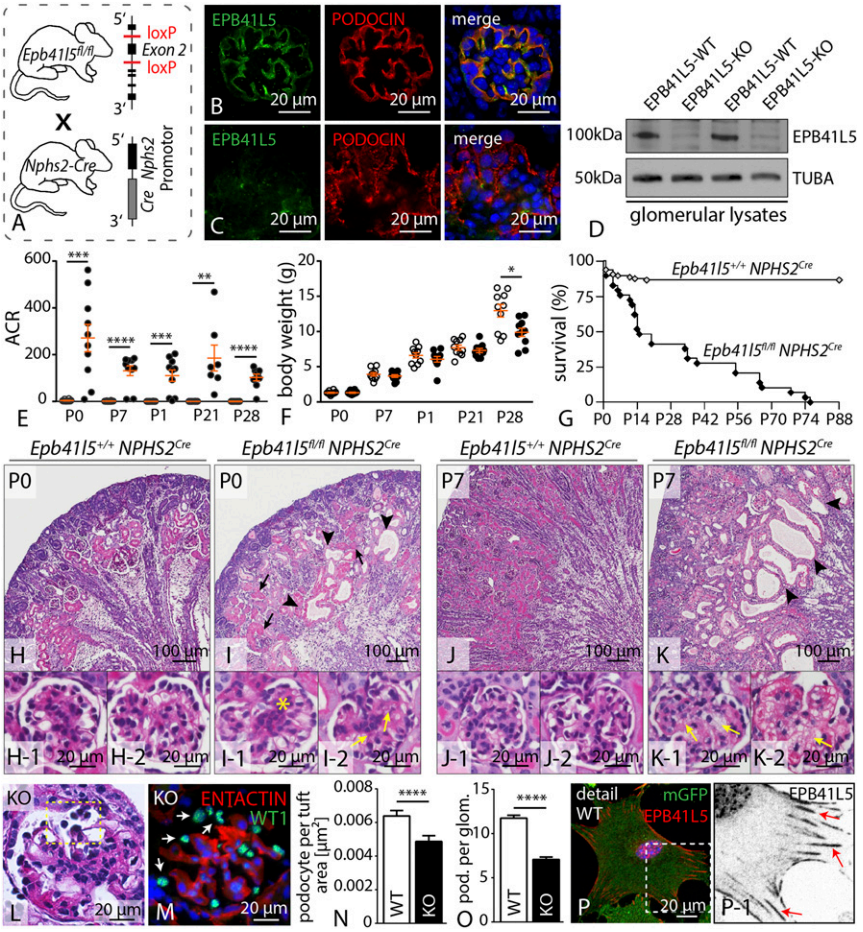

Fig. 3. Podocyte-specific knockout of *Epb41l5* causes nephrotic syndrome and lethality. (*A*) Schematic illustrating the generation of a podocyte-specific knockout mouse (*B* and *C*) Immunofluorescence staining confirmed that EPB41L5 protein is not detectable in the podocyte compartment in respective knockout mice. (*D*) Western blot on glomerular lysates from either control or respective knockout animals revealed that EPB41L5 protein is completely abolished. (*E* and *F*) Proteinuria measurements demonstrate a drastic increase of proteinuria in *Epb41l5* knockout animals beginning at P0 (at least $n = 7$; Dataset S3), accompanied by decreased body weight gain (at least $n = 10$ animals per group; *SI Appendix*, Dataset S3). (*G*) Kaplan-Meier analysis indicated premature death of *Epb41l5* knockout animals (at least n = 15; Dataset S3). (*H–K*) Histology of wild-type and *Epb41l5*$^{fl/fl}$**NPHS2*^{Cre} kidney sections revealed proteinaceous casts (black arrows), dilated tubules (black arrowheads), mesangial proliferation (yellow asterisk), and mesangiolysis (yellow arrows). (*L–O*) PAS and immunofluorescence staining for WT-1 demonstrated detachment of podocytes in *Epb41l5* knockout animals. Quantification of WT-1-positive cells in KO animals at 3 wk of age ($n = 3$ animals for each genotype; Dataset S3). (*P*) EPB41L5 localized in a typical FA pattern in primary wild-type podocytes (white box indicates zoom-in; red arrows indicate FAs). ACR, albumin to creatinine ratio.

immortalized human podocyte cell lines. After validation of specific gRNAs for the human EPB41L5 locus (targeting exon 2), we transfected immortalized human podocytes and isolated isogenetic clones. These clones were subsequently sequenced for deleterious mutations, and knockout efficiency was finally confirmed with Western blot (Fig. 4 *A* and *B* and *SI Appendix*, Fig. S13). As FAs are critically involved in dynamic cell–ECM interactions, we further tested for migration behavior and cellular adhesion in wild-type and respective knockout clones. Here, two independent *EPB41L5* knockout clones showed a pronounced defect in migration, as well as adhesion, when plated on collagen IV-coated ECM substratum (Fig. 4 *C–E* and *SI Appendix*, Fig. S13). The observation of impaired migration and adhesion implicated potential dysfunction in FA dynamics as a result of loss of EPB41L5. Therefore, we assessed cellular spreading and detected significant impairment of *EPB41L5* knockout clones, especially in early phases (Fig. 4 *F* and *G*), although there were no obvious differences under steady-state conditions (Fig. 4*G* and *SI Appendix*, Fig. S13 and S14). To validate the specificity of the observed phenotypes, we performed rescue experiments expressing full-length EPB41L5 in knockout clones. Here, we observed that reexpression of EPB41L5 leads to an amelioration of the spreading defect in EPB41L5 knockout cells (Fig. 4*H* and *SI Appendix*, Fig. S13). Analysis of FA morphology under dynamic conditions revealed a major proportion of immature FAs in *EPB41L5* knockout clones compared with wild-type controls (Fig. 4 *I–K*). Similar observations were also made in conditions of acute FA disassembly and reassembly via application of the myosin II inhibitor blebbistatin (24). Here, wild-type cells recovered faster and more efficiently, reflected by an increased amount of maturated FAs after washout of blebbistatin (*SI Appendix*, Fig. S14). These findings highlight the critical role of EPB41L5 for FA assembly and maturation. Because EPB41L5 appeared in a typical FA localization pattern in vivo and in vitro (Figs. 2 and 3*P*), we aimed to identify potential FA interaction partners of EPB41L5 via GST pull-down experiments. Here, we observed that the C-terminal part of EPB41L5 (encompassing amino acids 385–733; Fig. 4 *L* and *M*) interacted with PAXILLIN, whereas other bona fide FA components such as INTEGRIN-beta1 showed an interaction with neither the C-term nor the FERM-domain of EPB41L5 (Fig. 4*M* and *SI Appendix*, Fig. S14). In agreement with these data, localization studies demonstrated a clear colocalization of the C-terminal part of EPB41L5 with PAXILLIN at steady state and in spreading cells (Fig. 4 *N–Q*). Interestingly, a pronounced accumulation at the leading edge of spreading cells was observed for the C-terminal part of EPB41L5, together with PAXILLIN accumulating in nascent FAs (Fig. 4*Q* and *SI Appendix*, Fig. S14). In contrast, the FERM domain containing truncation showed a distinct localization pattern at the lamellum of spreading cells (Fig. 4*P*). These observations imply that the C-terminal part of EPB41L5 is not only interacting with PAXILLIN but also might be responsible for the localization toward the leading edge during cellular spreading.

EPB41L5-Mediated Cell Spreading Depends on Actomyosin Contractility. The process of cell spreading is being powered by contractile processes involving the actomyosin cytoskeleton (25). We observed that EPB41L5 predominantly accumulated at FA initiation sites, and also to the leading edge of cells in very early spreading phases (Fig. 5*A*). In addition, spreading *EPB41L5* KO cells exhibited a misconfigured cellular morphology characterized by the appearance of multiple pseudopods (Fig. 5 *B–D* and *SI Appendix*, Fig. S15), suggesting an impaired actomyosin regulation. We therefore hypothesized an active role for EPB41L5 in regulating the actomyosin machinery. In agreement with this hypothesis, preincubation of wild-type cells with inhibitors of actomyosin contractility phenocopied spreading and morphological defects of EPB41L5 KO cells (Fig. 5 *E–I* and *SI Appendix*, Fig. S15). The specificity of the pseudopod phenotype could be confirmed by rescue experiments, where reexpression of full-length EPB41L5 resulted in a significant reduction of pseudopod formation in respective knockout cells during spreading (Fig. 5*J*). Life imaging microscopy revealed that pseudopods are actively generated structures, characterized by a rather unorganized actin cytoskeleton and only small FAs (Fig. 5 *K–N* and *SI Appendix*, Fig. S15 and Movies S1–S5). In line with these observations, loss of EPB41L5 resulted in decreased levels of p-MLC specifically at the leading edge of spreading cells (Fig. 5 *O–Q*), accompanied by altered localization of MYOSIN-II (*SI Appendix*, Fig. S16). These findings were furthermore corroborated by Western blot experiments of either spreading or steady-state cells (Fig. 5 *R* and *W*). Again, reexpression of full-length EPB41L5 could reverse the reduced levels of p-MLC at the leading edge in EPB41L5 knockout cells (Fig. 5*S* and *SI Appendix*, Fig. S16). Because the activation mode of the actomyosin cytoskeleton is mainly regulated by of GTPases such as RhoA or Rac1 (26), we quantified for active levels of those. RhoA and Rac1 are either inactive (GDP-bound state) or active (GTP-bound state). Interestingly, we observed that EPB41L5 knockout cells exhibited lower levels of active RhoA during spreading, whereas at the same time, increased levels of active Rac1 were detected (Fig. 5 *T* and *U* and *SI Appendix*, Fig. S16). These findings indicate that loss of EPB41L5 results in a reciprocal activation of the GTPases RhoA and Rac1, finally leading to decreased actomyosin contractility. Remarkably, we also observed a pronounced accumulation of Rac1 in pseudopods of EPB41L5 knockout cells, potentially implying that Rac1 activation might account for this phenotype (Fig. 5*V*). Furthermore, *EPB41L5* knockout cells exhibited a much higher sensitivity toward myosin inhibition, characterized by altered cellular morphology (*SI Appendix*, Fig. S16). Together, these data indicated a clear correlation among the loss of EPB41L5, impaired actomyosin function, and defective cell spreading.

EPB41L5 Regulates Actomyosin Contractility via ARHGEF18. To understand the potential mechanisms of EPB41L5 in regulating the actomyosin machinery, we reanalyzed our initial in vivo iTRAQ proteomics approach and screened for podocyte-enriched GEFs as potential direct regulators of actomyosin contractility. Using this targeted approach, we identified the RhoGEF ARHGEF18, similar to EPB41L5, as a highly and specifically enriched podocyte candidate protein (Fig. 6 *A* and *F*). Previously, ARHGEF18 has been implicated in cell shape modulation by regulating myosin activity (27). To further characterize a potential interaction of both proteins, we performed coimmunoprecipitation assays and could demonstrate that ARHGEF18 precipitated EPB41L5 (Fig. 6*B*). Moreover, endogenous pull-down experiments using a specific antibody for ARHGEF18 revealed efficient precipitation of EPB41L5 in immortalized human podocytes (Fig. 6*C*). To better characterize this association, a set of complementary truncations for EPB41L5 was generated. Here, only the FERM domain containing truncations showed an efficient association with ARHGEF18 (Fig. 6*D* and *SI Appendix*, Fig. S17). These findings were corroborated by the use of GST-tagged recombinant protein versions for the FERM-/FERM-FA, full-length as well as C-terminal part of EPB41L5 in endogenous pull-down assays (Fig. 6*E* and *SI Appendix*, Fig. S17). In line with our iTRAQ proteomics data set, ARHGEF18 was strongly detected in podocytes in vivo, with a rather prominent perinuclear, as well as distinct basal, localization pattern (Fig. 6*F* and *SI Appendix*, Fig. S18). Similar to EPB41L5, ARHGEF18 was highly enriched at the leading edge of spreading podocytes (Fig. 6*G*). In agreement with the decreased p-MLC level (Fig. 5 *O–Q*), ARHGEF18 localization was reduced at the leading edge (Fig. 6 *H* and *I*) of *EPB41L5* KO cells. These data collectively indicated that EPB41L5 might be required to recruit ARHGEF18 to the leading edge as a prerequisite for actomyosin activation. To further corroborate the function of ARHGEF18 in podocytes, we used siRNA to generate

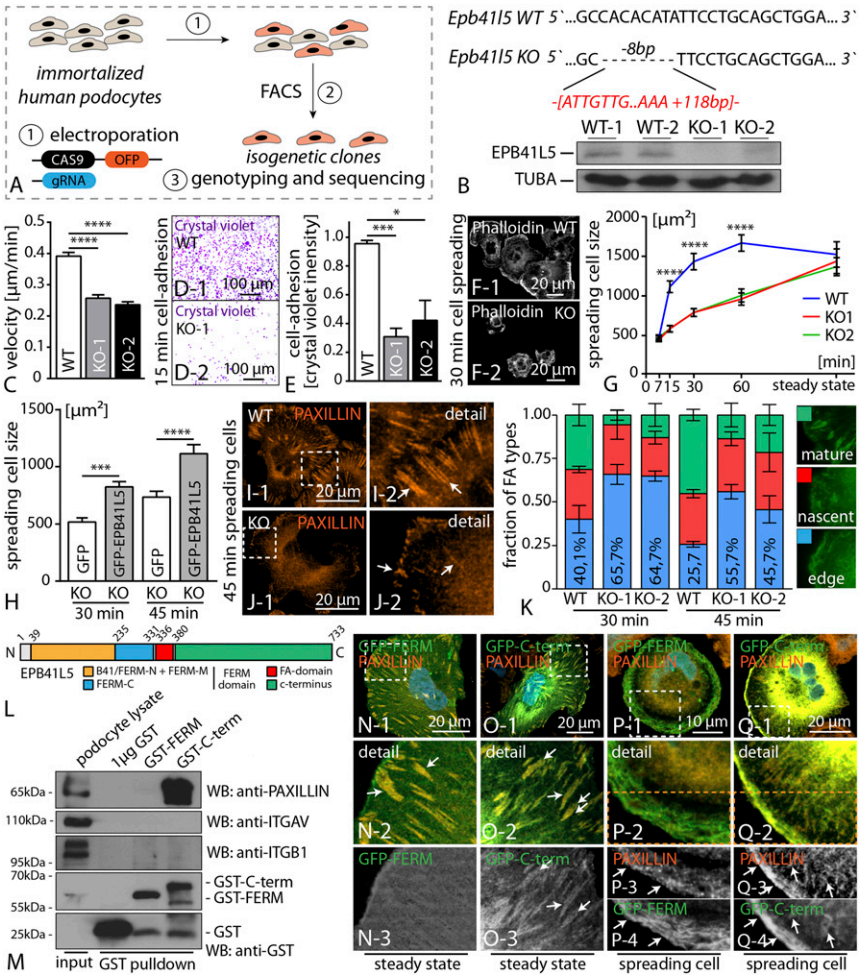

Fig. 4. EPB41L5 controls FA maturation and cellular spreading. (*A*) Schematic depicting the generation strategy of *EPB41L5* knockout using Crispr/CAS9 genome editing. (*B*) Exemplary Sanger sequencing results illustrating two different mutations in one podocyte clone. Western blot confirmed the absence of EPB41L5. (*C*) Single-cell migration analysis demonstrated a decreased migratory speed in *EPB41L5* knockout clones ($n = 86$ cells over three independent experiments; Dataset S3). (*D* and *E*) Decreased adhesion of EPB41L5 knockout cells ($n = 3$; Dataset S3). (*F* and *G*) Impaired cell spreading of knockout cells compared with wild-type controls ($n = 3$; Dataset S3). (*H*) Reexpression of full-length EPB41L5 ameliorated the spreading defect in EPB41L5 knockout cells (at least 70 cells were analyzed over three independent experiments; Dataset S3). (*I–K*) Quantification of FA subtypes in *EPB41L5* knockout cells demonstrated more immature FAs (>400 cells analyzed; Dataset S3). (*L*) Schematic depicting the domain structure of EPB41L5. (*M*) GST-pull-down experiments revealed that only the C-terminal part of EPB41L5 is required for association with the FA molecule PAXILLIN. (*N–Q*) Expression of GFP-tagged versions of C-terminal or FERM-domain truncations highlighted the FA localization pattern for the C-terminal part (Q3-4; white arrows indicate colocalization with PAXILLIN). FACS, fluorescence-activated cell sorting.

knockdown of ARHGEF18. Remarkably, loss of ARHGEF18 phenocopied the spreading defects of *EPB41L5* knockout cells and was accompanied by decreased levels of p-MLC (Fig. 6 *J–O* and *SI Appendix*, Fig. S18).

ECM Influences EPB41L5 Mediated Phenotypes. From hereditary collagenopathies, it is evidenced that podocytes rely on collagen type IV interactions to maintain their mechanical stress resistance and filter function (28, 29). Therefore, we speculated that the EPB41L5-mediated regulatory networks stabilizing cell function, cell adhesion, and contractility might be specifically influenced by the ECM composition. In fact, observed phenotypes resulting from loss of EPB41L5 were influenced by provided ECM ligands and respective concentrations. Wild-type cells showed a dose-dependent increase in cell size during spreading on either collagen IV or fibronectin. Although the spreading defects of EPB41L5 KO cells persisted on all collagen IV concentrations, high concentrations of fibronectin could ameliorate the spreading defect of EPB41L5 KO cells and prevented the hypersensitivity toward myosin II inhibitors (Fig. 7 *A–C* and *E–J* and *SI Appendix*, Fig. S19), suggesting that EPB41L5, in addition to its general effect on FA maturation, is particularly required for the execution of collagen IV-mediated outside-in signaling. In agreement, quantification of active RhoA for cells spreading on fibronectin revealed almost equalized levels of EPB41L5 KO cells compared with wild-type cells, in contrast to persistently diminished RhoA activation on collagen IV (Figs. 7*D* and 5*T*). To elucidate this phenomenon, we performed quantitative SILAC (stable isotope labeling with amino acids in cell culture)-based focal adhesome proteomics (30), in which enriched and chemically cross-linked FA complexes are analyzed using mass spectrometry (30). Strikingly, we detected that loss of EPB41L5 modulated the composition of the focal adhesome, most prominently on the level integrin receptors such as INTEGRIN-beta1 (Fig. 7 *K* and *L* and Dataset S2). Although not primarily detected in the MS data set (most probably because of sensitivity issues), we could reveal that the collagen-binding INTEGRIN-alpha2 also concordantly exhibited lower levels in the focal adhesome fraction of EPB41L5-depleted cells (Fig. 7*L*). Thus, EPB41L5 appears to be required for efficient collagen IV-mediated outside-in signaling in podocytes.

Discussion

Modulation and regulation of adhesion represents a fundamental mechanism in epithelial cell biology (9). Interaction of epithelial cells with the surrounding ECM or the underlying basement membrane is mediated by different adhesion receptors such as integrin adhesion complexes (9, 31). In this study, we focused on the adhesome of podocytes. The medical relevance of podocyte adhesion is underlined by the fact that podocyte detachment is a key factor for chronic kidney disease progression (32–34). Previous studies mainly focused on key components of the integrin adhesome, such as different integrin subunits or central signaling proteins such as ILK and TALIN (11, 12, 15). Despite those previous advances, there is still only limited knowledge about cell type-specific modulation of cell adhesion and contractility. To identify potential podocyte-inherent adhesome modulators, we performed an in vivo screening approach

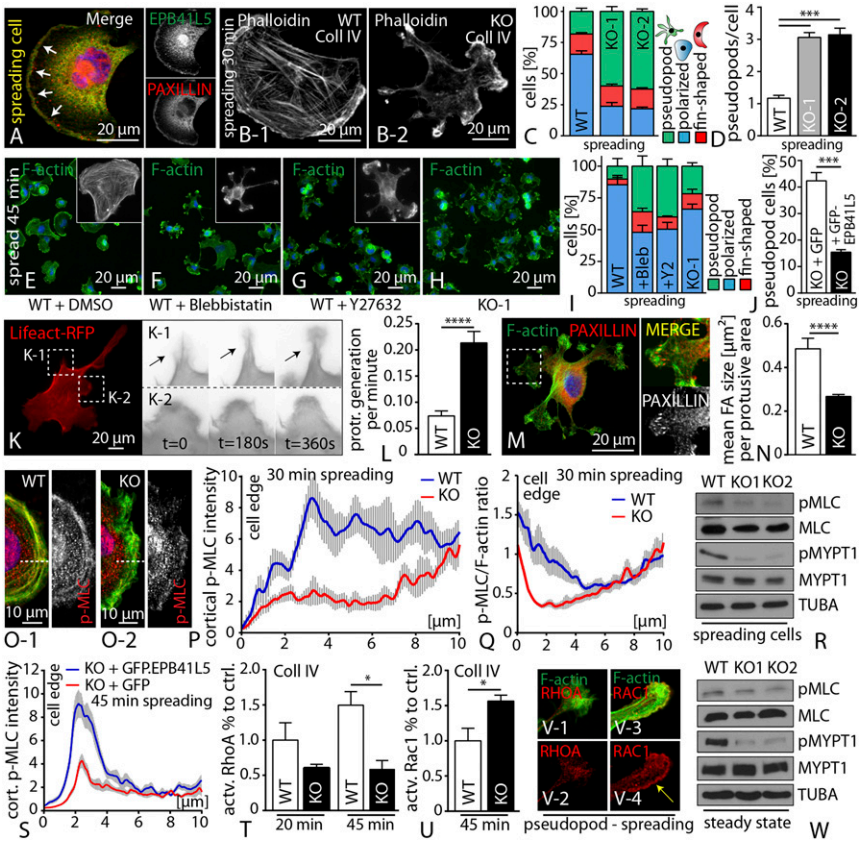

Fig. 5. EPB41L5-mediated cell spreading depends on actomyosin contractility. (*A*) During initial phases of spreading, EPB41L5 colocalized with PAXILLIN at nascent adhesion initiation sites. (*B–D*) Loss of EPB41L5 resulted in the formation of pseudopodial protrusions (>100 cells over three experiments, 30 min spreading; Dataset S3). (*E–I*) Treatment of wild-type cells with blebbistatin or Y27632 promoted the formation of pseudopods (at least n = 50 cells over three experiments, 45 min spreading; Dataset S3). (*J*) Reexpression of full-length EPB41L5 ameliorated the pseudopod phenotype in EPB41L5 knockout (>100 cells over three experiments; 30 min spreading; Dataset S3). (*K* and *L*) Life imaging of EPB41L5 knockout cells revealed pseudopod formation as an active process (Dataset S3). (*M* and *N*) FA morphology is shifted toward smaller adhesion sites in pseudopod protrusions (12 WT and 23 KO cells were analyzed; Dataset S3). (*O–Q*) Analysis for P-MLC showed decreased levels at the leading edge of spreading *EPB41L5* KO cells (n = 10 over two experiments; Dataset S3). (R) Western blot on spreading wild-type and EPB41L5 KO cells showed decreased levels of P-MLC as well as P-MYPT. (*S*) Reexpression of full-length EPB41L5 restores p-MLC levels at the leading. (*T* and *U*) Quantification of active GTPase levels during cell spreading showed decreased active RhoA and increased active Rac1 levels in knockout cells (n = 3; Dataset S3). (*V*) RAC1 and RHOA immunofluorescence in knockout pseudopods. (*W*) Western blot on steady state EPB41L5 KO cells showed decreased levels of P-MLC, as well as P-MYPT.

and identified the FERM domain protein EPB41L5 as a highly selectively expressed FA component of podocytes (Figs. 1 and 2). The importance of EPB41L5 for podocyte function was furthermore supported by the profound phenotype of conditional knockout mice and striking down-regulation in a series of human glomerular disease conditions, as well as experimental mouse and cell models (Fig. 3 and *SI Appendix*, Figs. S5, S6, and S20). More recently, it was demonstrated that loss of TALIN (genetic deletion and experimental stress models), a well-established core focal adhesome component, results in a dramatic podocyte phenotype characterized by massive proteinuria, as well as consecutive development of glomerular sclerosis (15). Interestingly, TALIN-deficient podocytes exhibited a mild adhesion and spreading defect, but a predominant misconfiguration of the actin cytoskeleton. In contrast, EPB41L5 mainly influenced dynamic cellular functions such as spreading and adhesion via titration of the actomyosin machinery (Figs. 4 and 5).

The EPB4.1 protein family is involved in cellular morphogenesis, and EPB41L5 was particularly investigated in terms of apicobasal polarity establishment via interaction with CRUMBS in early development (35, 36). Previous work demonstrated that EPB41L5 was required during early embryo gastrulation, which seemed to be partially a result of EPB41L5-dependent FA modulation and cell–cell contact establishment via cadherins (37). On the basis of our observations, we here propose that EPB41L5 mainly influences the maturational phase of FAs, implicating that decreased tension or traction might attribute for the detachment of podocytes, as evidenced in the EPB41L5 knockout model (Figs. 3 and 4). The actomyosin cytoskeleton is involved in multiple cellular functions ranging from migration, to cellular morphogenesis, to adhesion (38). Although ARHGEF18 was previously implicated in controlling cell migration, our data now indicate that the RhoGEF ARHGEF18 acts downstream of EPB41L5-regulated cellular spreading in the cell-specific context of podocytes (Fig. 6) (39). In agreement with the known role of ARHGEF18 as a RHOGEF activator for RhoA, we observed decreased levels of active RhoA and concomitantly increased activation of Rac1 in EPB41L5 knockout cells during spreading (Fig. 5). Although hyperactivation of Rac1 is an accepted pathogenetic model in podocyte disease verified by several independent studies (40, 41), there is an ambiguous perception regarding the role of RhoA. Nevertheless, an emerging body of evidence supports the concept of a required balance of these GTPases to maintain cellular function (42). Therefore, our findings exemplify the interdependent and reciprocal interplay of small GTPases and demonstrate their essential role for podocyte spreading and adhesion maturation (Fig. 6).

The disturbed activity of the actomyosin cytoskeleton also contributes to the prominent feature of active pseudopod formation in EPB41L5 knockout cells during spreading (Fig. 5 and Movies S1–S5). Pseudopods represent a specialized cellular protrusion type mainly observed in chemotactic cell types, and Rac1 activation has been shown to be involved in the initiation and propagation of pseudopod formation (43). In light of this, the pseudopod phenotype of EPB41L5 knockout cells might reflect the disturbed balance of GTPase activation and insufficient FA maturation, ultimately culminating in the generation of numerous unstable cellular projections. A very recent study could demonstrate that stabilization of the actin cytoskeleton via application of a small molecule affecting the DYNAMIN structure resulted in prevention of progressive proteinuria in a series of genetic and toxic podocyte stress models. These observations underlined the importance of the actin cytoskeleton as a common final pathway of podocyte injury (44, 45). Our data now extend these observations and identify with EPB41L5, a podocyte-specific upstream link from the adhesion machinery to the regulation of the cytoskeleton. As FAs are known to transmit outside-in-signals, this also raised the possibility of potential sensing

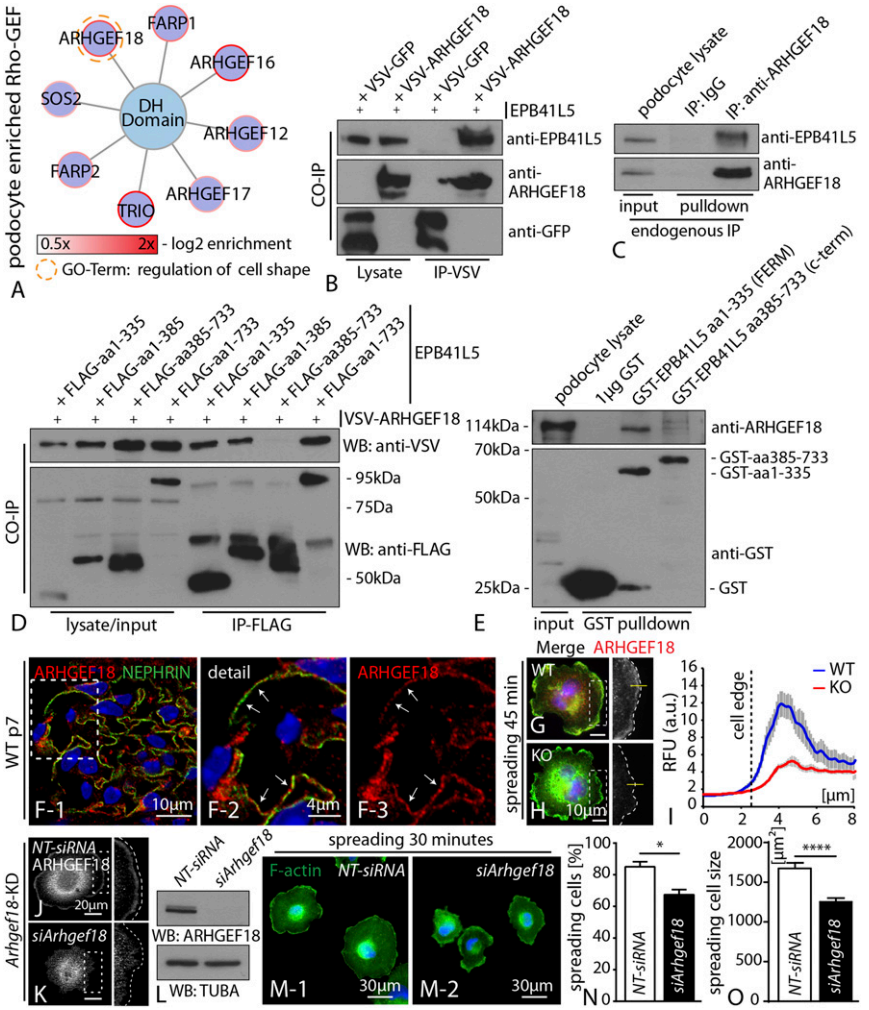

Fig. 6. EPB41L5 regulates actomyosin contractility via ARHGEF18. (*A*) Subanalysis of the in vivo iTRAQ proteomics dataset for DH domain containing small GTPases. ARHGEF18 showed a high enrichment score, as well as involvement in cell shape regulation. (*B*) Coimmunoprecipitation between epitope-tagged EPB41L5 and ARHGEF18. (*C*) Endogenous EPB41L5 was precipitated via pull-down with an antibody directed against ARHGEF18, IgG was included as a control. (*D*) A series of different EPB41L5 truncations (all epitope tagged) were used to map the association with ARHEF18; here only the FERM domain containing truncations precipitated ARHGEF18. (E) GST-tagged recombinant protein versions of either FERM domain or C-terminal truncations of EPB41L5 were used in endogenous pull-down experiments. Only the FERM domain containing truncation precipitated ARHGEF18. (*F*) Immunofluorescence staining for ARHGEF18 on murine adult glomeruli revealed colocalization with the podocyte marker NEPHRIN (boxed regions indicate zoomed-in detail). (*G–I*) Immunofluorescence staining for ARHGEF18 on cells, while spreading revealed localization toward the leading edge. Quantification of immunofluorescence intensities across the cell border indicated decreased levels ARHGEF18 in KO cells (at least 20 cells per genotype were analyzed over two independent experiments). (*J–L*) siRNA-mediated knockdown of *ARHGEF18* in immortalized human podocytes, as confirmed via immunofluorescence and Western blot. (*M–O*) Knockdown of ARHGEF18 resulted in significant impairment of early spreading on collagen IV surfaces (at least 100 cells per condition were analyzed and averaged over three independent experiments; Dataset S3).

properties of the EPB41L5 FA-associated complex. Interestingly, we detected an EPB41L5-dependent alteration of the focal adhesome composition (Fig. 7 and Dataset S2). Altogether, these changes might serve as a possible explanation for differential ECM response properties because of the loss of EPB41L5 (Fig. 7). In fact, our findings suggest the physiological GBM composition influences the EPB41L5 associated signaling response (Fig. 7), suggesting collagenopathies such as Alport syndrome specifically contribute to changes in podocyte adhesion signaling, finally leading to podocyte loss and progressive kidney disease (29).

Collectively, we describe here comprehensive adhesome mapping of podocytes in vivo as a unique model to study the requirements of FAs under enormous physical forces. On the basis of the identification of EPB41L5, we describe a cell-inherent concept of FA maturational control via integration of the actomyosin cytoskeleton and context-dependent ECM sensing, which is required to maintain the integrity of the kidney filtration barrier (Fig. 7).

Materials and Methods

Please refer to *SI Appendix* for complete details of materials and methods, as well as all supplemental figures.

Animals. EPB41L5 knockout mice were generated as described in *SI Appendix, Materials and Methods*. All animal experiments were approved by local authorities (Regierungspräsidium Freiburg, Freiburg 79106 – approval number G10/39).

MS Analysis. Detailed description of isolation and analysis is described in *SI Appendix, Materials and Methods*. All analyzed data are provided as Datasets S1 and S2.

Super Resolution Microscopy. Super resolution microscopy was performed in principle, as previously described (22). Further details are provided in the *SI Appendix, Materials and Methods*.

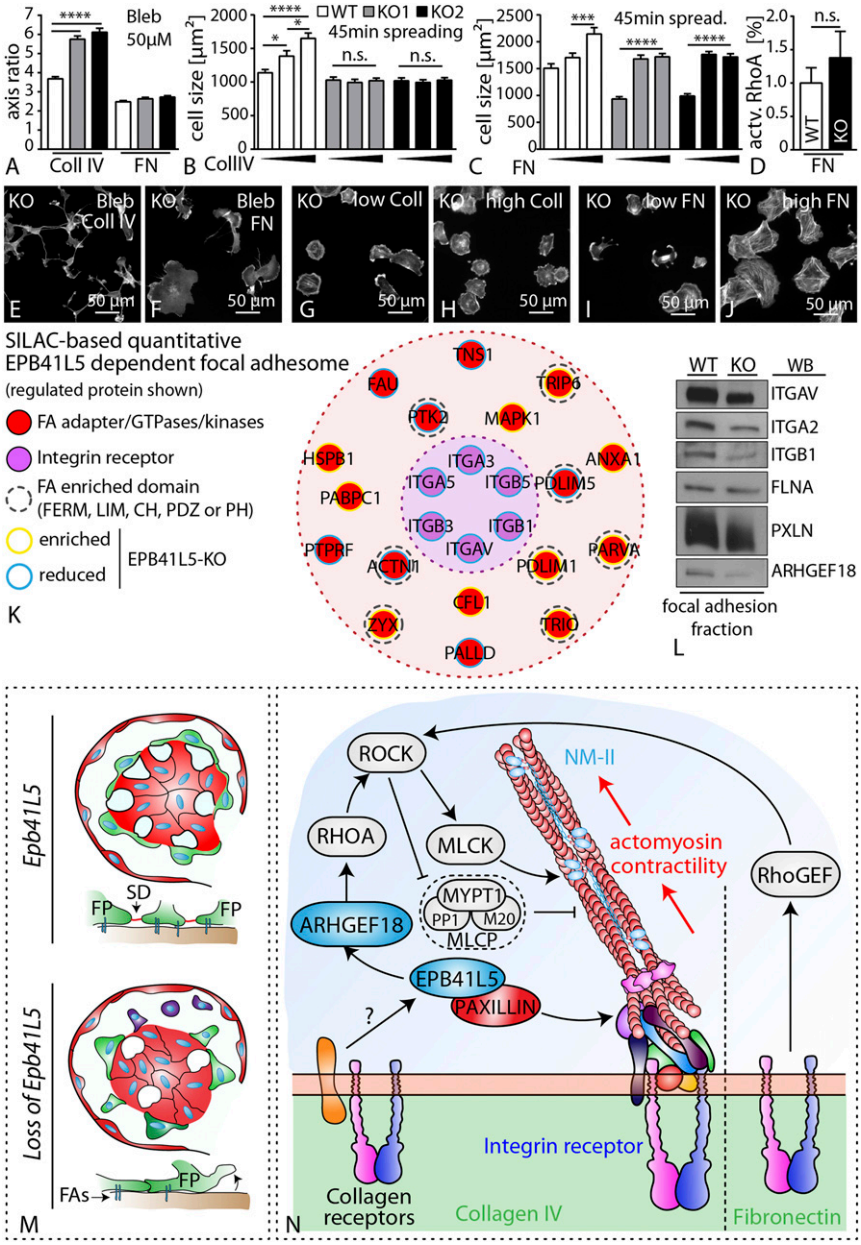

Fig. 7. ECM influences EPB41L5-mediated phenotypes. (*A*) Cell morphology assessed as major–minor axis quantification revealed altered morphological appearance of *EPB41L5* KO cells on collagen compared with fibronectin conditions (at least 145 cells were analyzed, averaged more than three independent experiments; Dataset S3). (*B*, *C*, *D–J*) *EPB41L5* KO clones show defective ECM sensing on collagen IV coated substratum. In contrast, increasing concentrations of the ECM ligand fibronectin led to improved spreading in respective KO clones (at least 100 cells per genotype and condition were analyzed, averaged over three independent experiments; Dataset S3). (*K*) Map of SILAC-based quantitative EPB41L5 dependent focal adhesome. (*L*) Western blot confirmation of focal adhesome fraction revealing balanced levels for PAXILLIN, whereas ITGB1, ITGA2, and also ARHGEF18 showed decreased intensity compared with the wild-type. (*M*) Schematic summarizing the phenotypic features of the EPB41L5 knockout characterized by foot process effacement and pronounced podocyte detachment. (*N*) EPB41L5 modulates actomyosin contractility via direct recruitment of the small GTPase ARHGEF18, and thereby influences FA maturation. This process is influenced via ECM composition and potential regulatory roles mediated by collagen receptors. Coll, collagen IV; ECM, extracellular matrix; FA, focal adhesion; FN, fibronectin, NM-II, nonmuscle myosin 2; SD, slit diaphragm; SILAC, stable isotope labeling by amino acids in cell culture.

CAS9-Mediated Knockout in Immortalized Human Podocytes. Detailed description of gRNA design, transfection, and isolation of respective clones is provided in the *SI Appendix*, *Materials and Methods*.

Statistics and Reproducibility. Data are expressed as mean ± SEM, if not stated otherwise. Based on data distribution (normal vs. nonnormal distribution), paired Student´s *t* test, one-way ANOVA (multiple comparison test, Tukey), or nonparametric two-tailed Mann-Whitney tests were performed. Experiments were not randomized or blinded. Statistical significance was defined as $*P < 0.05$, $**P < 0.01$, $***P < 0.001$, and $****P < 0.0001$; NS, not significant. Number of independent experiments and total amount of analyzed cells are stated either in the figure legends or listed in Dataset S3.

ACKNOWLEDGMENTS. We thank Charlotte Meyer, Christina Engel, Betina Kiefer, Barbara Joch, Helga Schachner, and Elisabeth Wiesner for expert technical assistance. In addition, we would like to express our gratitude to all members of our laboratories for helpful discussions and support, especially Ketan Patel for carefully reading the manuscript. We would also like to thank Ronald Roepman for generously providing antibodies and serum against EPB41L5. We thank Cristina Has for providing ITGalpha2 antibodies. This study was supported by the German Research Foundation: collaborative research

centers (CRC) 1140 (to T.B.H. and F.G.) and CRC 992 (to T.B.H.), Heisenberg program (T.B.H.), HU 1016/5-1 and HU 1016/8-1 (to T.B.H.); by the European Research Council (T.B.H.), and by the H2020-IMI2 consortium Biomarker Enterprise to Attack Diabetic Kidney Disease (BEAt-DKD) (115974 to T.B.H.); by the Bundesministerium für Bildung und Forschung, STOP Fokale Segmentale Glomerulosklerose (BMBF-STOP-FSGS) 01GM1518C (T.B.H.); by the Excellence Initiative of the German Federal and State Governments (GSC-4, Spemann Graduate School, C.S. and T.B.H.; BIOSS, T.B.H.; and the Freiburg Institute for Advanced Studies, T.B.H. and J.D.); by the Else Kröner Fresenius Stiftung, Nierenfunktionsstörungen als Komplikation von Systemerkrankungen (NAKSYS) (C.S., M.R., and T.B.H.) and Molekulare und Translationale Forschung in Freiburg – Verantwortungsvolle Ausbildung Tatkräftige Ermutigung (MOTIVATE) (D.S.); by the German Society of Nephrology (C.S.); and we gratefully acknowledge the financial support from the Ministerium für Innovation, Wissenschaft und Forschung des Landes Nordrhein-Westfalen, the Senatsverwaltung für Wirtschaft, Technologie und Forschung des Landes Berlin, and the Bundesministerium für Bildung und Forschung (to L.K., R.P.Z., and A.S.).

1. Faul C, Asanuma K, Yanagida-Asanuma E, Kim K, Mundel P (2007) Actin up: Regulation of podocyte structure and function by components of the actin cytoskeleton. *Trends Cell Biol* 17:428–437.
2. Grahammer F, Schell C, Huber TB (2013) The podocyte slit diaphragm–from a thin grey line to a complex signalling hub. *Nat Rev Nephrol* 9:587–598.
3. Simons M, Hartleben B, Huber TB (2009) Podocyte polarity signalling. *Curr Opin Nephrol Hypertens* 18:324–330.
4. Aaltonen P, Holthöfer H (2007) The nephrin-based slit diaphragm: New insight into the signalling platform identifies targets for therapy. *Nephrol Dial Transplant* 22: 3408–3410.
5. Kriz W, Lemley KV (2015) A potential role for mechanical forces in the detachment of podocytes and the progression of CKD. *J Am Soc Nephrol* 26:258–269.
6. Lennon R, Randles MJ, Humphries MJ (2014) The importance of podocyte adhesion for a healthy glomerulus. *Front Endocrinol (Lausanne)* 5:160.
7. Sachs N, Sonnenberg A (2013) Cell-matrix adhesion of podocytes in physiology and disease. *Nat Rev Nephrol* 9:200–210.
8. Hynes RO (1992) Integrins: Versatility, modulation, and signaling in cell adhesion. *Cell* 69:11–25.
9. Winograd-Katz SE, Fässler R, Geiger B, Legate KR (2014) The integrin adhesome: From genes and proteins to human disease. *Nat Rev Mol Cell Biol* 15:273–288.
10. Has C, et al. (2012) Integrin α3 mutations with kidney, lung, and skin disease. *N Engl J Med* 366:1508–1514.
11. Kanasaki K, et al. (2008) Integrin beta1-mediated matrix assembly and signaling are critical for the normal development and function of the kidney glomerulus. *Dev Biol* 313:584–593.
12. Pozzi A, et al. (2008) Beta1 integrin expression by podocytes is required to maintain glomerular structural integrity. *Dev Biol* 316:288–301.
13. El-Aouni C, et al. (2006) Podocyte-specific deletion of integrin-linked kinase results in severe glomerular basement membrane alterations and progressive glomerulosclerosis. *J Am Soc Nephrol* 17:1334–1344.
14. Sachs N, et al. (2006) Kidney failure in mice lacking the tetraspanin CD151. *J Cell Biol* 175:33–39.
15. Tian X, et al. (2014) Podocyte-associated talin1 is critical for glomerular filtration barrier maintenance. *J Clin Invest* 124:1098–1113.
16. Boerries M, et al. (2013) Molecular fingerprinting of the podocyte reveals novel gene and protein regulatory networks. *Kidney Int* 83:1052–1064.
17. Akilesh S, et al. (2011) Arhgap24 inactivates Rac1 in mouse podocytes, and a mutant form is associated with familial focal segmental glomerulosclerosis. *J Clin Invest* 121: 4127–4137.
18. Horton ER, et al. (2015) Definition of a consensus integrin adhesome and its dynamics during adhesion complex assembly and disassembly. *Nat Cell Biol* 17:1577–1587.
19. Schell C, Wanner N, Huber TB (2014) Glomerular development–shaping the multicellular filtration unit. *Semin Cell Dev Biol* 36:39–49.
20. Huber TB, et al. (2009) Loss of podocyte aPKClambda/iota causes polarity defects and nephrotic syndrome. *J Am Soc Nephrol* 20:798–806.
21. Hartleben B, et al. (2012) Role of the polarity protein Scribble for podocyte differentiation and maintenance. *PLoS One* 7:e36705.
22. Suleiman H, et al. (2013) Nanoscale protein architecture of the kidney glomerular basement membrane. *eLife* 2:e01149.
23. Schell C, et al. (2013) N-wasp is required for stabilization of podocyte foot processes. *J Am Soc Nephrol* 24:713–721.
24. Kuo JC, Han X, Hsiao CT, Yates JR, 3rd, Waterman CM (2011) Analysis of the myosin-II-responsive focal adhesion proteome reveals a role for β-Pix in negative regulation of focal adhesion maturation. *Nat Cell Biol* 13:383–393.
25. Wolfenson H, Iskratsch T, Sheetz MP (2014) Early events in cell spreading as a model for quantitative analysis of biomechanical events. *Biophys J* 107:2508–2514.
26. Lawson CD, Burridge K (2014) The on-off relationship of Rho and Rac during integrin-mediated adhesion and cell migration. *Small GTPases* 5:e27958.
27. Nakajima H, Tanoue T (2011) Lulu2 regulates the circumferential actomyosin tensile system in epithelial cells through p114RhoGEF. *J Cell Biol* 195:245–261.
28. Suh JH, Miner JH (2013) The glomerular basement membrane as a barrier to albumin. *Nat Rev Nephrol* 9:470–477.
29. Meehan DT, et al. (2009) Biomechanical strain causes maladaptive gene regulation, contributing to Alport glomerular disease. *Kidney Int* 76:968–976.
30. Schiller HB, Friedel CC, Boulegue C, Fässler R (2011) Quantitative proteomics of the integrin adhesome show a myosin II-dependent recruitment of LIM domain proteins. *EMBO Rep* 12:259–266.
31. Geiger T, Zaidel-Bar R (2012) Opening the floodgates: Proteomics and the integrin adhesome. *Curr Opin Cell Biol* 24:562–568.
32. Kriz W, Hähnel B, Hosser H, Rösener S, Waldherr R (2014) Structural analysis of how podocytes detach from the glomerular basement membrane under hypertrophic stress. *Front Endocrinol (Lausanne)* 5:207.
33. Kobayashi N, et al. (2015) Podocyte injury-driven intracapillary plasminogen activator inhibitor type 1 accelerates podocyte loss via uPAR-mediated β1-integrin endocytosis. *Am J Physiol Renal Physiol* 308:F614–F626.
34. Potla U, et al. (2014) Podocyte-specific RAP1GAP expression contributes to focal segmental glomerulosclerosis-associated glomerular injury. *J Clin Invest* 124:1757–1769.
35. Gosens I, et al. (2007) FERM protein EPB41L5 is a novel member of the mammalian CRB-MPP5 polarity complex. *Exp Cell Res* 313:3959–3970.
36. Laprise P, et al. (2009) Yurt, Coracle, Neurexin IV and the Na(+),K(+)-ATPase form a novel group of epithelial polarity proteins. *Nature* 459:1141–1145.
37. Hirano M, Hashimoto S, Yonemura S, Sabe H, Aizawa S (2008) EPB41L5 functions to post-transcriptionally regulate cadherin and integrin during epithelial-mesenchymal transition. *J Cell Biol* 182:1217–1230.
38. Salbreux G, Charras G, Paluch E (2012) Actin cortex mechanics and cellular morphogenesis. *Trends Cell Biol* 22:536–545.
39. Terry SJ, et al. (2011) Spatially restricted activation of RhoA signalling at epithelial junctions by p114RhoGEF drives junction formation and morphogenesis. *Nat Cell Biol* 13:159–166.
40. Auguste D, et al. (2016) Disease-causing mutations of RhoGDIα induce Rac1 hyperactivation in podocytes. *Small GTPases* 7:107–121.
41. Yu H, et al. (2013) Rac1 activation in podocytes induces rapid foot process effacement and proteinuria. *Mol Cell Biol* 33:4755–4764.
42. Guilluy C, Garcia-Mata R, Burridge K (2011) Rho protein crosstalk: Another social network? *Trends Cell Biol* 21:718–726.
43. Li A, et al. (2011) Rac1 drives melanoblast organization during mouse development by orchestrating pseudopod- driven motility and cell-cycle progression. *Dev Cell* 21: 722–734.
44. Schiffer M, et al. (2015) Pharmacological targeting of actin-dependent dynamin oligomerization ameliorates chronic kidney disease in diverse animal models. *Nat Med* 21:601–609.
45. Gu C, et al. (2017) Dynamin autonomously regulates podocyte focal adhesion maturation. *J Am Soc Nephrol* 28:446–451.